Electronic supplementary information

Hydrothermally grown CdS nanograin-sensitized 1D Zr:Fe_2O_3/FTO photoanode for efficient solar-light-driven photoelectrochemical performance

Mahadeo A. Mahadik[§, a], Arunprabaharan Subramanian[§, a], Jungho Ryu[b], Min Cho[a, *] and Jum Suk Jang[a, *]

[a] Division of Biotechnology, Safety, Environment and Life Science Institute, College of Environmental and Bioresource Sciences, Chonbuk National University, Iksan 570-752, Republic of Korea.

[b] Mineral Resources Research Division, Korea Institute of Geoscience and Mineral Resources (KIGAM), Daejeon 305-350, Republic of Korea.

[§] Authors with equal contribution.

*Corresponding authors. Tel.: +82 63 850 0846; fax: +82 63 850 0834.
E-mail addresses: jangjs75@jbnu.ac.kr (J.S. Jang), cho317@ jbnu.ac.kr (Min Cho).

Table S1. Recent reports on photoelectrochemical performance of CdS/Fe_2O_3 photoanodes.

Year	Photoelectrode	Method	Electrolyte	Performance	Ref
2016	**CdS/1D $Zr:Fe_2O_3$ Nanorod arrays**	**Hydrothermal + Immersion**	**0.50 M Na_2S and 0.50 M Na_2SO_3**	**3.3 mA/cm^2 0.2 V versus Ag/AgCl**	**[Our work]**
2016	CdS /Ti-Fe_2O_3 2D nanosheets	Electrodeposition + Dipping	0.50 M Na_2S and 0.50 M Na_2SO_3	2.7 mA/cm^2 0.2 V versus Ag/AgCl	[1]
2016	Fe_2O_3/CdS co-sensitized TiO_2 nanotube arrays (TNA)	ultrasonic-assisted chemical bath deposition (CBD) method	0.35 M Na_2SO_3 + 0.25 M Na_2S.	0.904 mA/cm^2 (0.0 $V_{Ag/AgCl}$)	[2]
2015	mesoporous Fe_2O_3–CdS heterostructures	interfacial thermal decomposition +chemical bath deposition method	phosphate buffer saline (pH 7.4)	0.9 mA/cm^2 0.0 V (vs Ag/AgCl)	[3]
2013	3D hierarchical CdS/α-Fe_2O_3 heterojunction nanocomposites	facile chemical bath method	0.1 M Na_2SO_4	1.4 $\mu A/cm^2$ Vs saturated calomel electrode (SCE)	[13]

Table S2: Variation of crystallite size and micro strain according to the annealing at different temperatures.

$CdS/Zr:Fe_2O_3$	D (nm)	ε_μ ($\times 10^{-4}$)
As-grown	74.7	8.7
250 °C	69.7	9.3
350 °C	109.1	16.2
400 °C	77.4	12.0

Table S3: Comaprison of photoelectorchemical performance of annealed CdS/1D Zr:Fe_2O_3 heterostructured array at different experimentatal condition.

Electrode	Applied potential	Electrolyte	Performance
CdS/1D Zr:Fe_2O_3 annealed at 350 °C	(-0.3 $V_{Ag/AgCl}$)	0.1 M Na_2S + 0.02 M Na_2SO_3.	2.2 mA/cm^2
	(0.2 $V_{Ag/AgCl}$)	0.1 M Na_2S and 0.02 M Na_2SO_3	3.1 mA/cm^2
	(-0.3 $V_{Ag/AgCl}$)	0.5 M Na_2S and 0.5 M Na_2SO_3	3.0 mA/cm^2
	(0.2 $V_{Ag/AgCl}$)	**0.5 M Na_2S and 0.5 M Na_2SO_3**	**3.3 mA/cm^2**

Table S4: EIS fitting parameters of the bare 1D Zr:α-Fe_2O_3, CdS, and CdS/1D Zr:Fe_2O_3 heterostructured array deposited at various time intervals.

Samples/ Parameters	R_s Ω	R_2 Ω	R_3 Ω	$C_{[CPE1]}$ μF	$C_{[CPE2]}$ μF
1D Zr:Fe_2O_3	51	123	929	0.33	196
CdS	47	722	3681	3.2	5.3
10_CdS/1D Zr:Fe_2O_3	52	93	870	0.41	157
20_CdS/1D Zr:Fe_2O_3	42	87	618	0.6	229
30_CdS/1D Zr:Fe_2O_3	57	95	641	0.46	135
40_CdS/1D Zr:Fe_2O_3	89	144	643	0.31	150

Table S5: EIS fitting parameters of the bare CdS/1D Zr:Fe_2O_3 heterostructured array annealed at various temperatures.

Annealing temperature/ EIS parameters	R_s Ω	R_2 Ω	R_3 Ω	$C_{[CPE1]}$ μF	$C_{[CPE2]}$ μF
250 °C	96	24	840	0.28	1.9
300 °C	62	17	734	0.20	3.0
350 °C	63	14	664	0.20	3.1
400 °C	62	19	861	0.29	2.1

Table S6: EIS fitting parameters of the bare CdS coated Zr:α-Fe_2O_3, and 5, 10 mM $Ni(OH)_2$ loaded CdS coated Zr:Fe_2O_3 heterostructured array.

Sample/ parameters	R_s Ω	R_2 Ω	R_3 Ω	$C_{[CPE1]}$ μF	$C_{[CPE2]}$ μF
CdS/1D Zr:Fe_2O_3	63	14	664	0.20	3.1
5 mM $Ni(OH)_2$ loaded CdS/1D Zr:Fe_2O_3	124	7.5	700	17	34
10 mM $Ni(OH)_2$ loaded CdS/1D Zr:Fe_2O_3	99	7.4	883	0.24	33

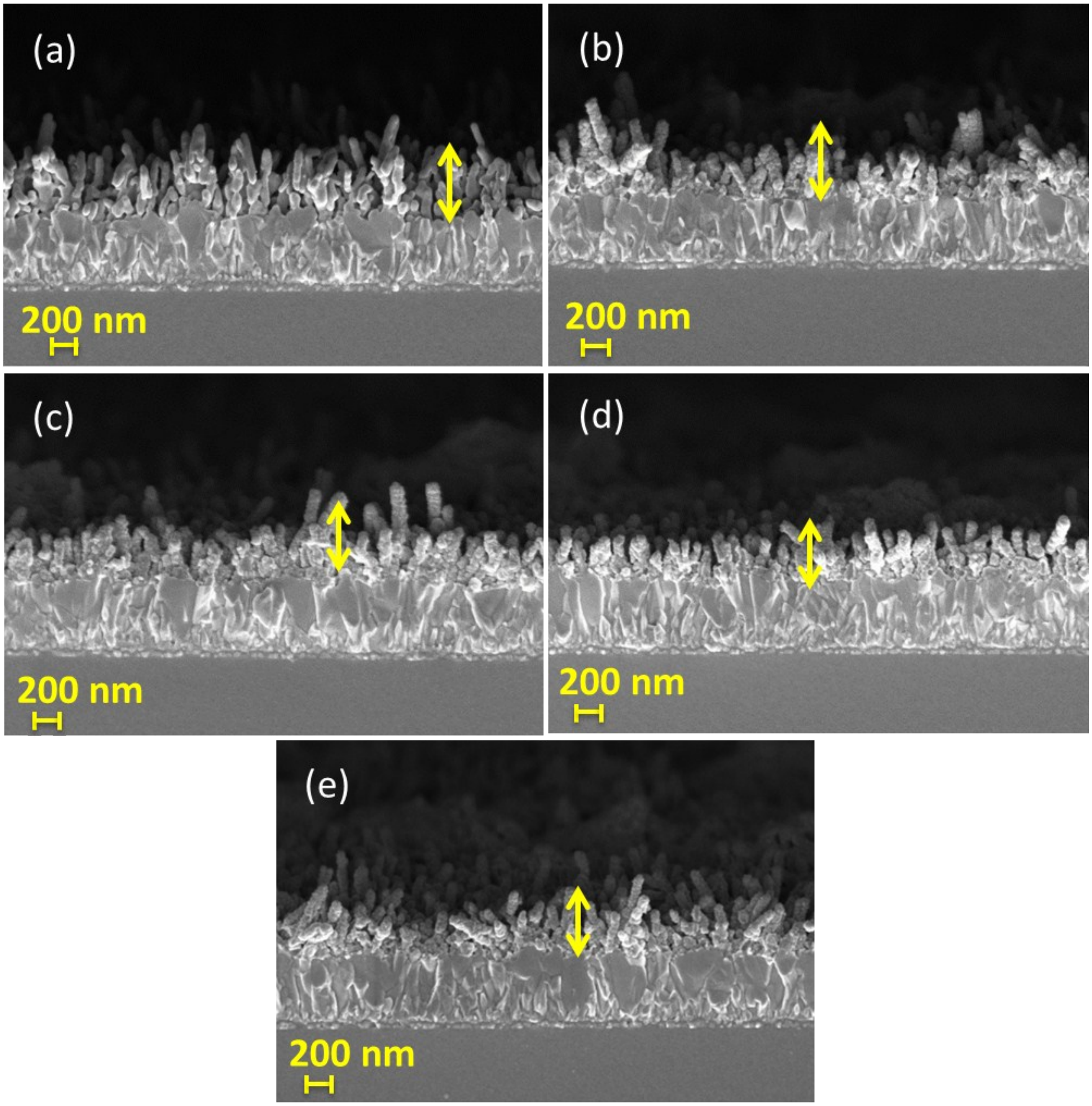

Fig. S1: FE-SEM cross-sectional images of (a) pristine 1D Zr:Fe_2O_3, and CdS deposited on 1D Zr:Fe_2O_3 for (b) 10 min, (c) 20 min, (d) 30 min, (e) 40 min, respectively.

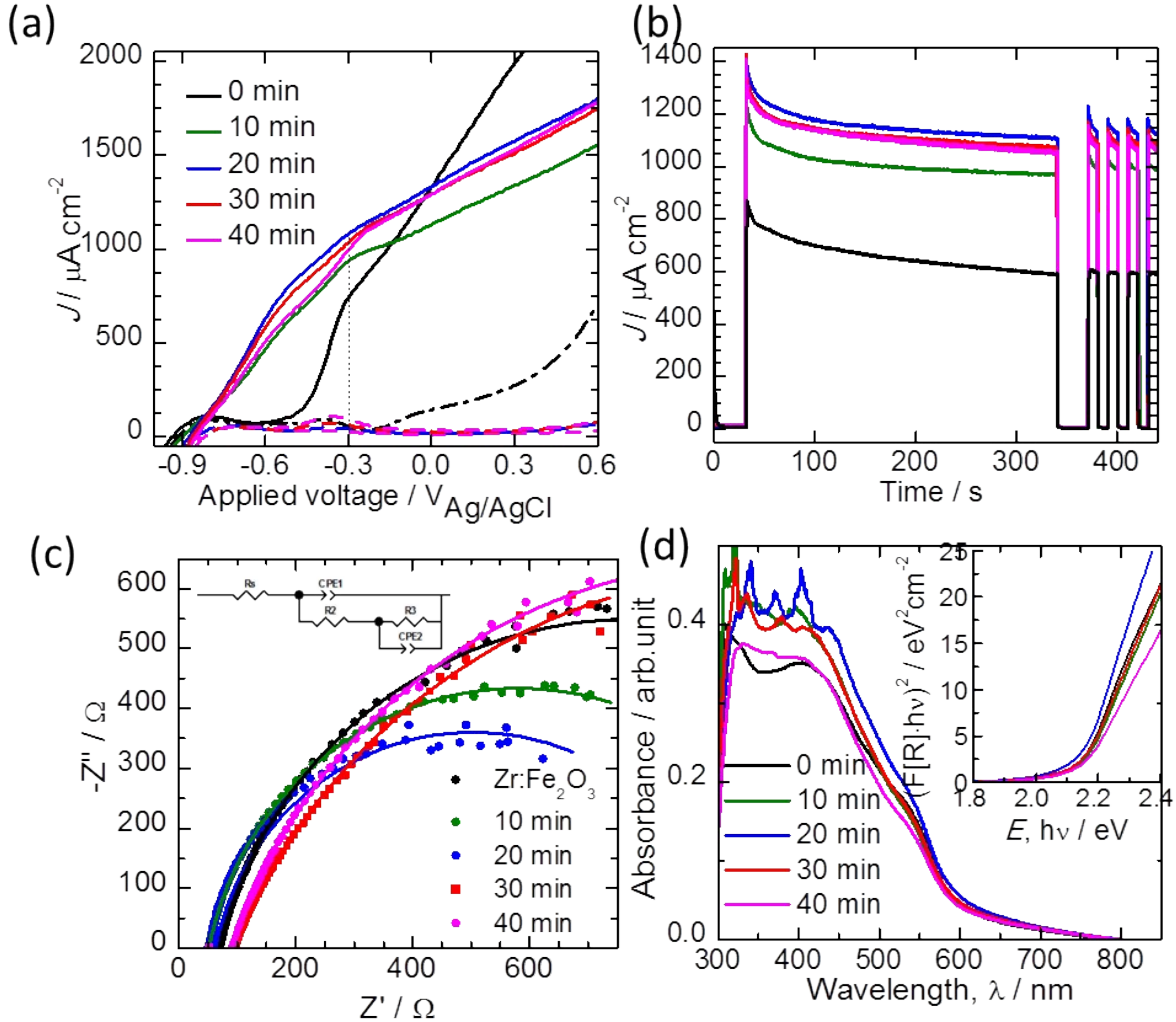

Fig. S2: (a) Current density-voltage characteristics (solid lines) and in the dark (dash lines) at a scan rate of 50 mVs^{-1}, (b) Potentiostatic photocurrent density-time characteristic, under simulated AM 1.5G illumination, (c) EIS spectrum of CdS/1D $Zr:Fe_2O_3$ (d) UV-Vis absorption spectrum for CdS/1D $Zr:Fe_2O_3$ deposited at (a), 10 min, 20 min, 30 min, and 40 min. Inset shows the corresponding band gaps.

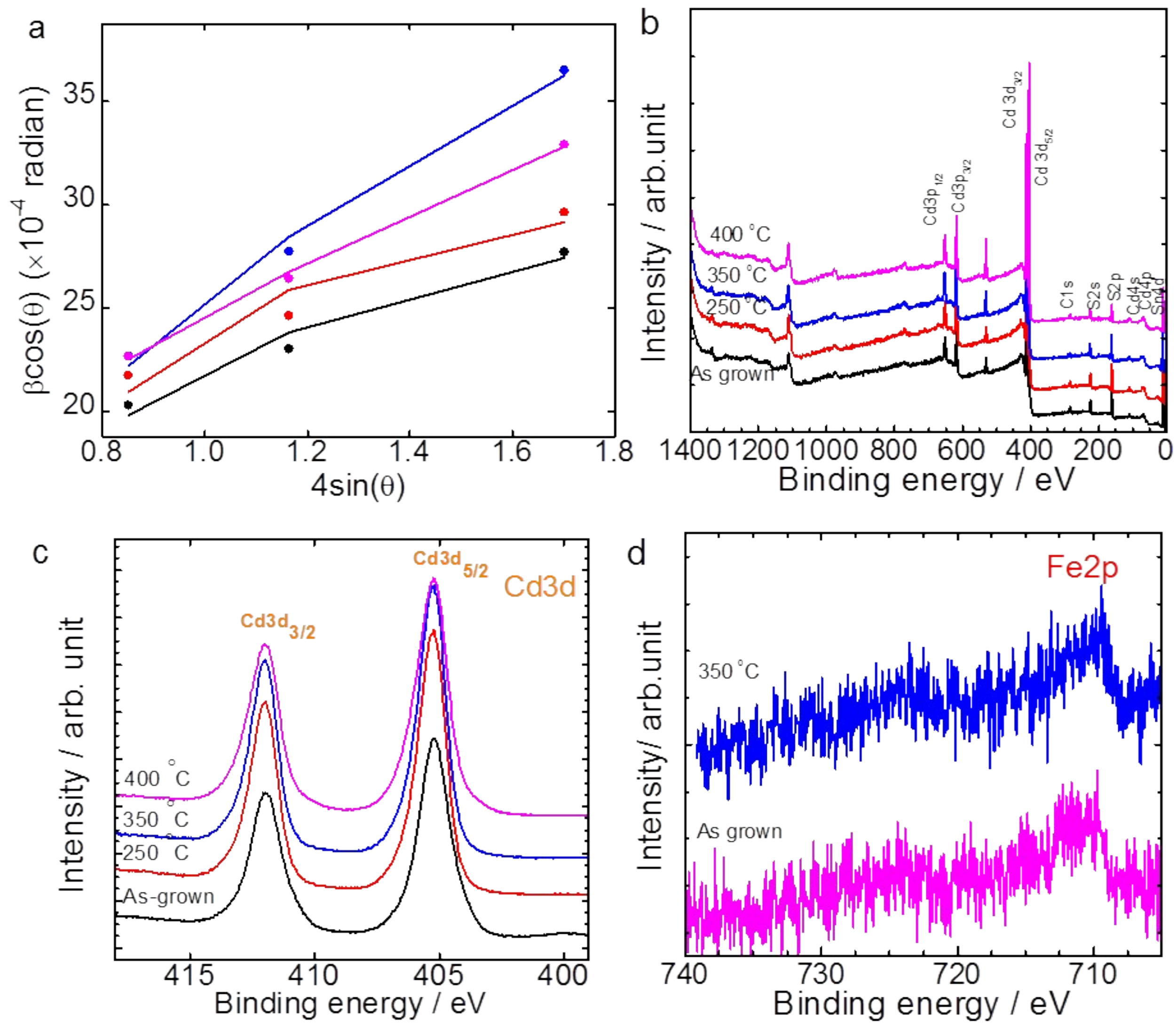

Fig. S3: (a) Williamson-Hall plot for the as-grown and the annealed CdS/1D Zr:Fe_2O_3 photoanodes, (b) XPS survey scan and (c,d) nanrrow scan spectra of Cd3d and Fe2p for CdS/1D Zr:Fe_2O_3 heterostructure photoanodes. The presence of Cd peaks (Cd $3d_{5/2}$ at 405.3 eV and Cd $3d_{3/2}$ at 411.9 eV) corresponds to the presence of the oxidation state +2 of Cd 3d in CdS[4-6].

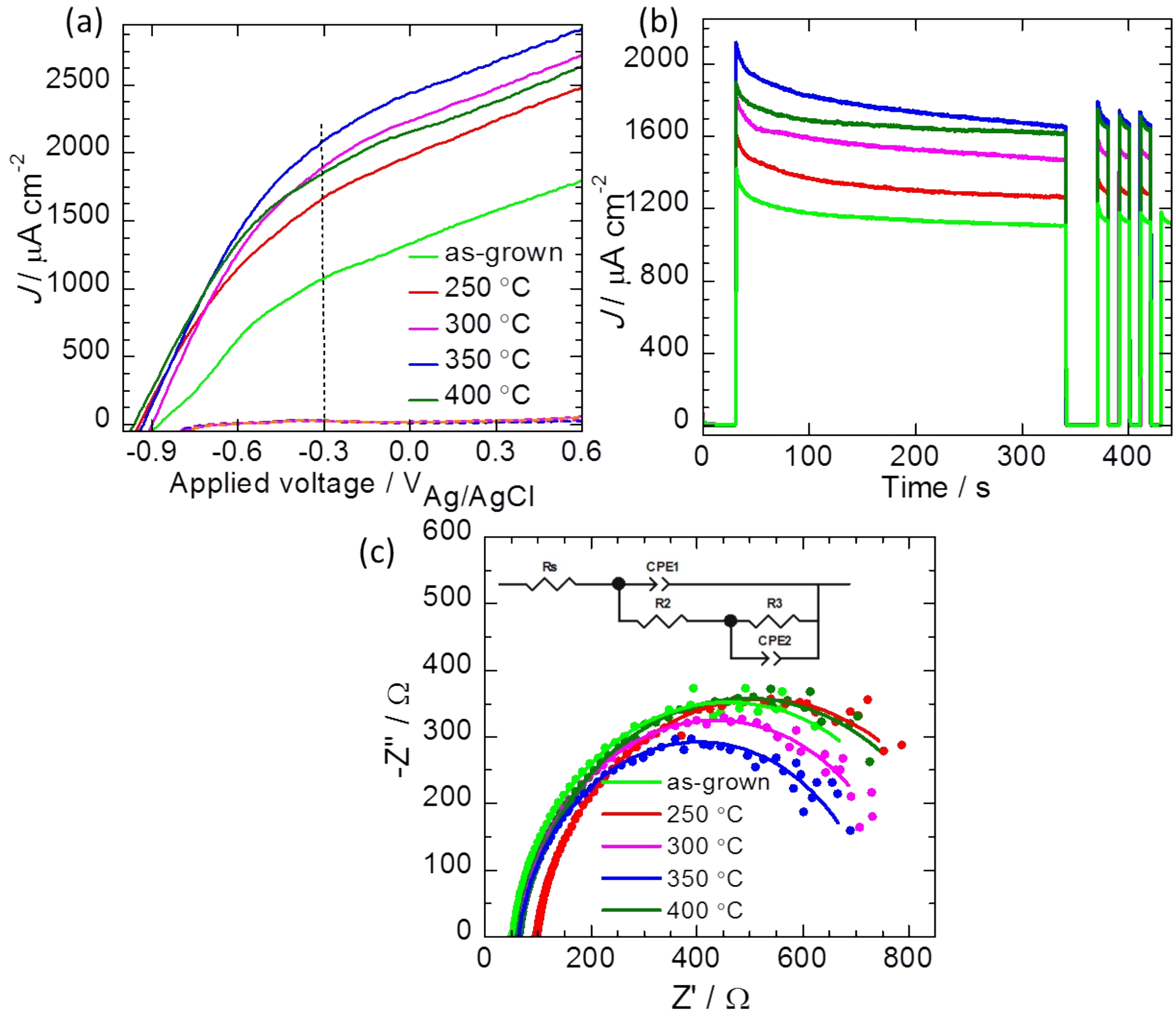

Fig. S4: (a) Current density-voltage characteristics (solid lines) and in the dark (dash lines), (b) Potentiostatic photocurrent density-time characteristic, (c) EIS specta under simulated AM 1.5G illumination for CdS/1D Zr:Fe_2O_3 annealed at different temperatures, Inset shows the simple equivalent circuit used to fit the EIS specta.

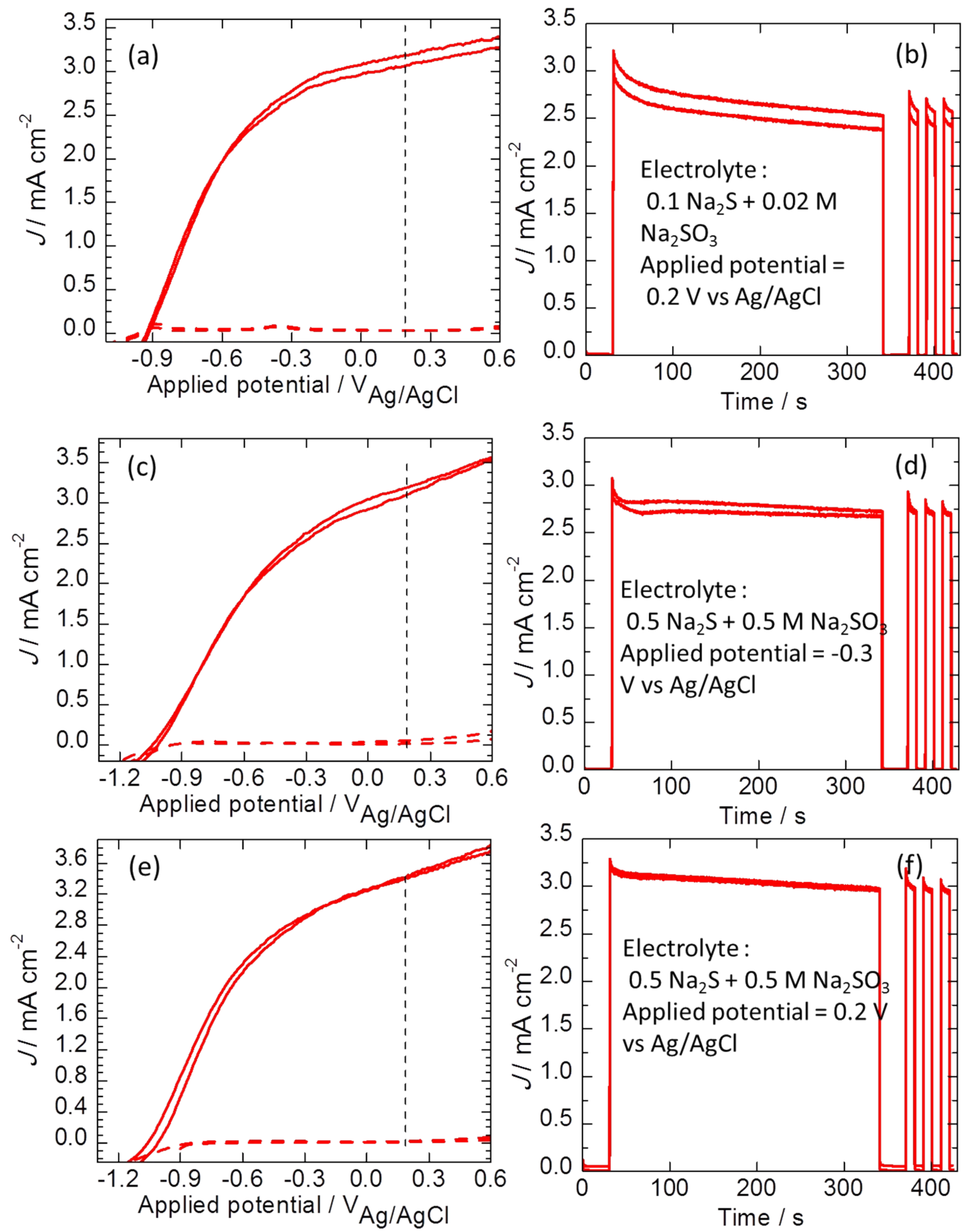

Fig. S5: Current density-voltage characteristics (a,c, e) and potentiostatic photocurrent density-time (b,d,f) characteristics of annealed CdS/1D Zr:Fe_2O_3 at different experimental conditions.

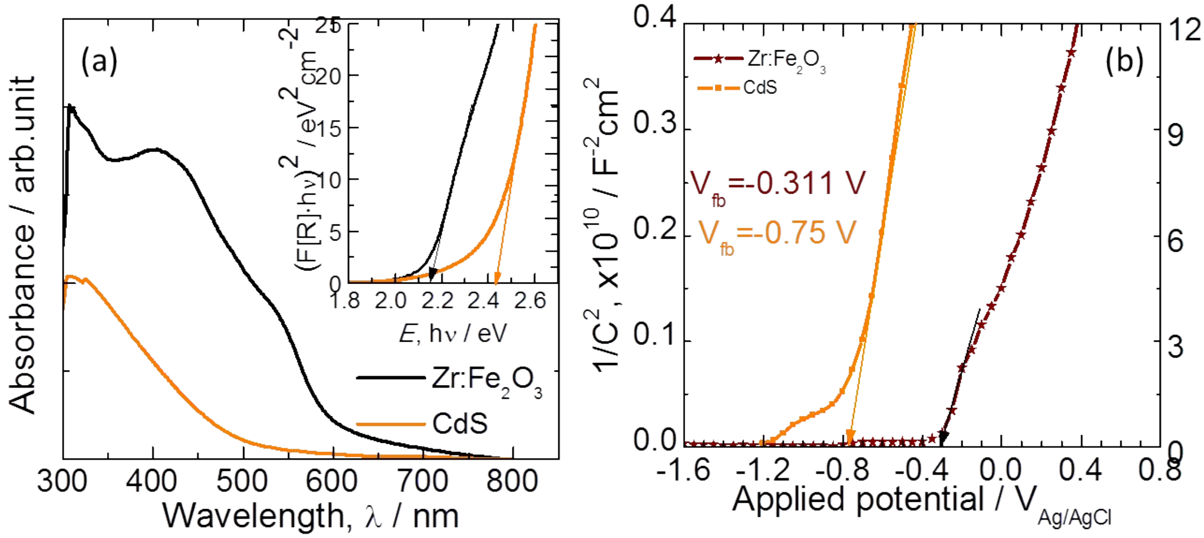

Fig. S6: (a) UV-Visible absorption spectrum. Inset shows the corresponding band gaps, (b) Mott-Schottky plots measured in a 0.1 M Na_2S + 0.02 M Na_2SO_3 electrolyte for bare CdS and 1D Zr:α-Fe_2O_3 on FTO.

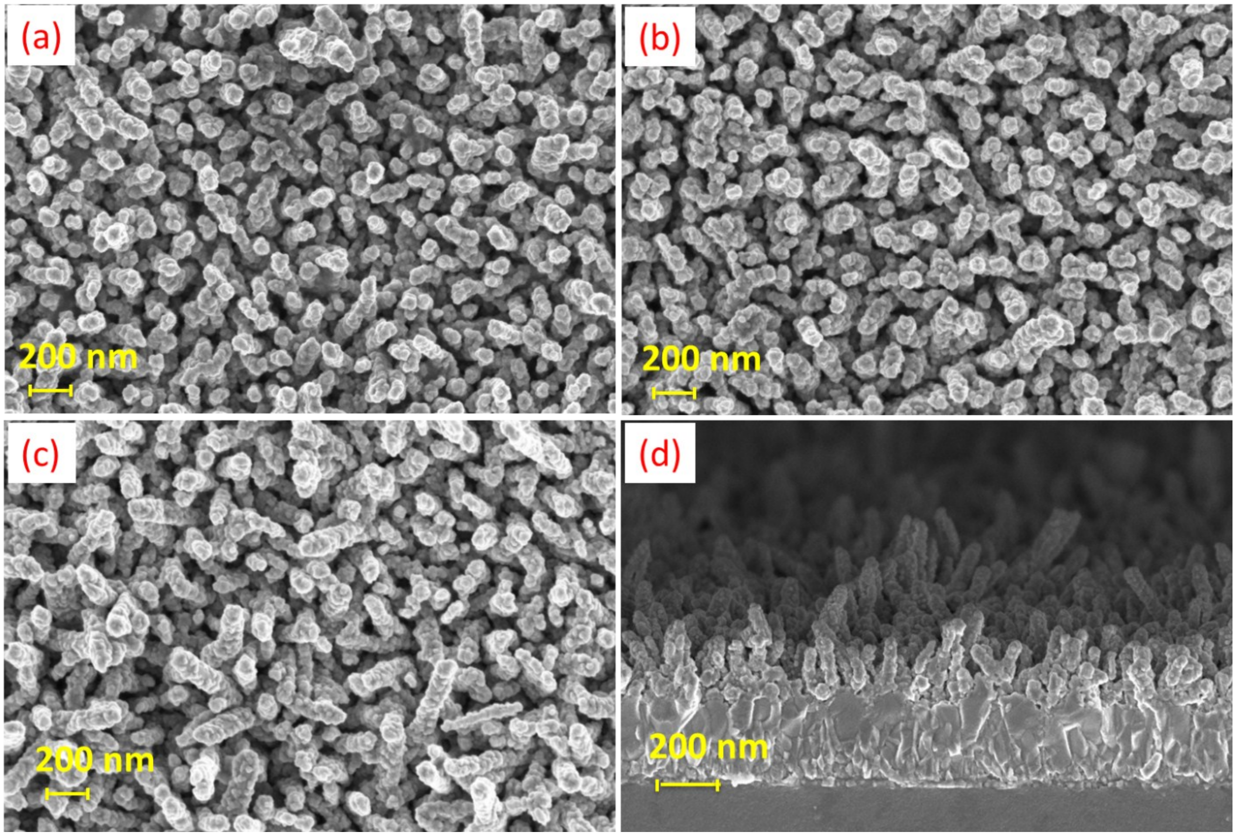

Fig. S7 Top-view FE-SEM images of (a) 2 mM, (b) 5 mM, (c) 10 mM, and (d) cross-sectional FE-SEM image of the 5 mM nickel precursor loaded on annealed CdS/1D Zr:Fe_2O_3.

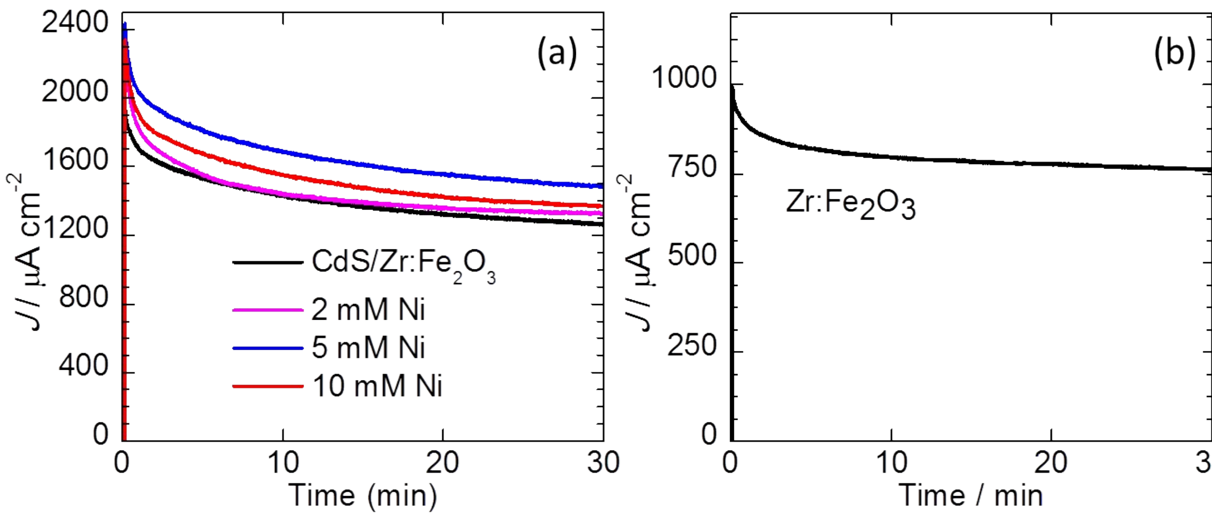

Fig. S8 Stability test of $Ni(OH)_2$/CdS/1D Zr:Fe_2O_3 ands pristine 1D Zr:α-Fe_2O_3 deposited on FTO substrates.

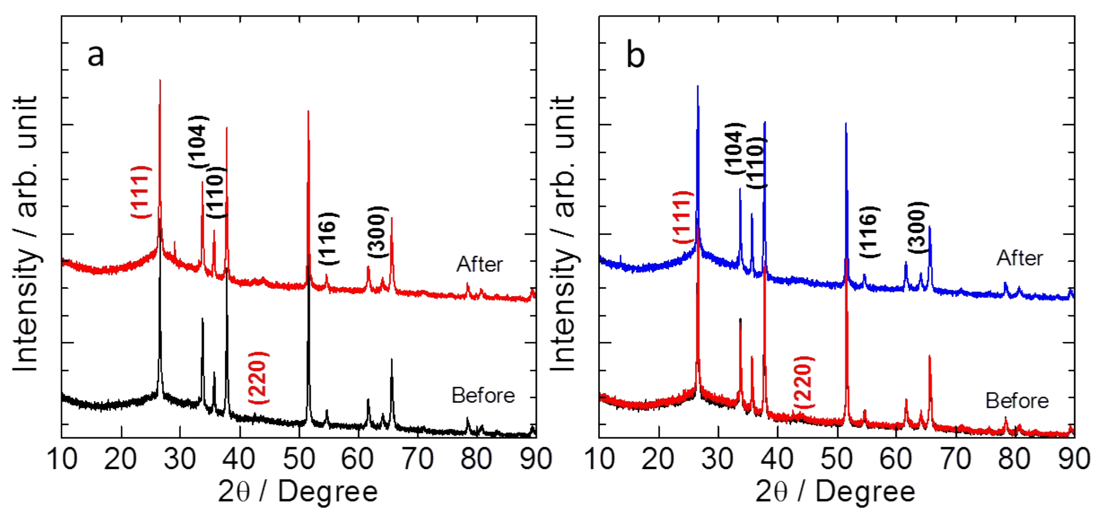

Fig. S9 XRD patterns of (a) CdS nanograin-sensitized 1D Zr:α-Fe_2O_3 and (b) $Ni(OH)_2$ loaded CdS nanograin-sensitized 1D Zr:α-Fe_2O_3 nanorod arryas before and after PEC measurements.

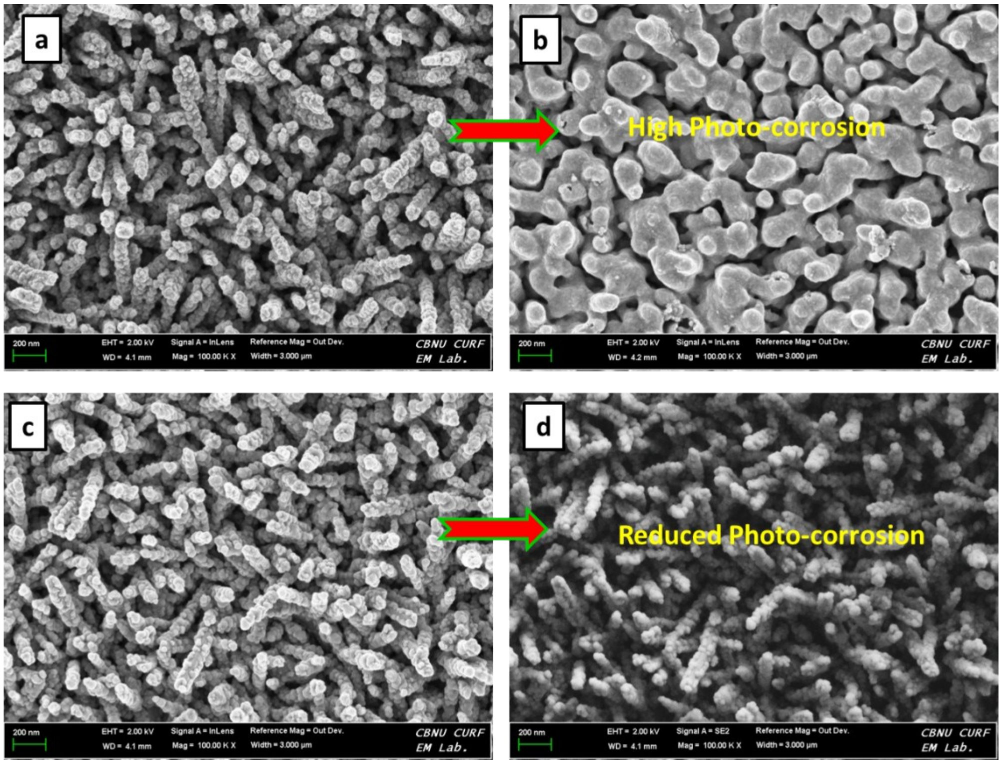

Fig. S10. FESEM of (a, c) CdS nanograin-sensitized 1D Zr:α-Fe_2O_3 and $Ni(OH)_2$ loaded CdS nanograin-sensitized 1D Zr:α-Fe_2O_3 nanorod arryas before PEC measurements and (b,d) are of after measurements.

Before PEC **After PEC**

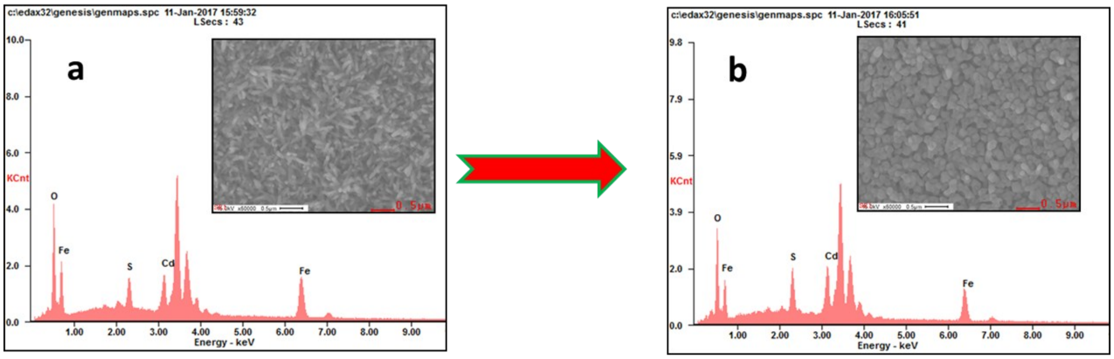

Element	Wt%	At%
OK	26.24	59.46
SK	07.81	08.83
CdL	33.97	10.96
FeK	31.98	20.76
Matrix	Correction	ZAF

Element	Wt%	At%
OK	27.02	59.47
SK	05.65	06.21
CdL	25.62	08.03
FeK	41.70	26.30
Matrix	Correction	ZAF

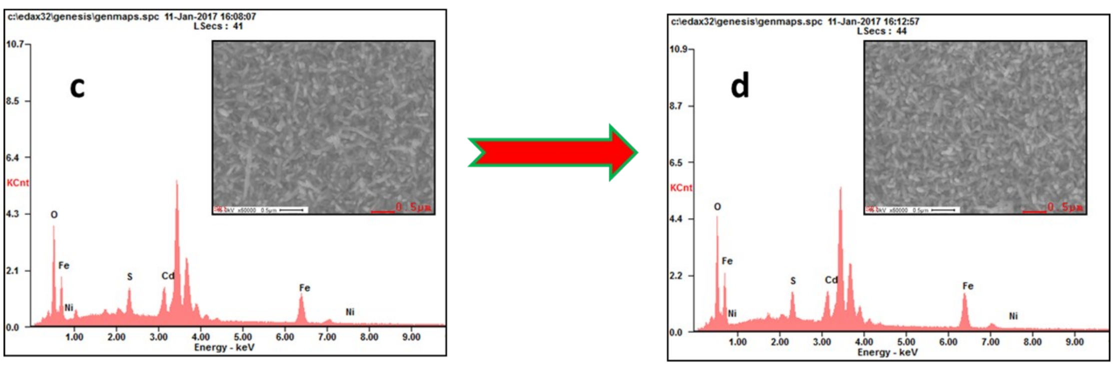

Element	Wt%	At%
OK	29.95	63.18
SK	06.14	06.46
CdL	27.04	08.12
FeK	35.69	21.57
NiK	01.18	00.68
Matrix	Correction	ZAF

Element	Wt%	At%
OK	28.60	61.23
SK	05.67	06.06
CdL	24.57	07.49
FeK	40.09	24.59
NiK	01.08	00.63
Matrix	Correction	ZAF

Fig. S11. EDS of (a, c) CdS nanograin-sensitized 1D Zr:α-Fe_2O_3 and $Ni(OH)_2$ loaded CdS nanograin-sensitized 1D Zr:α-Fe_2O_3 nanorod arryas before PEC measurements and (c,d) are the after measurements.

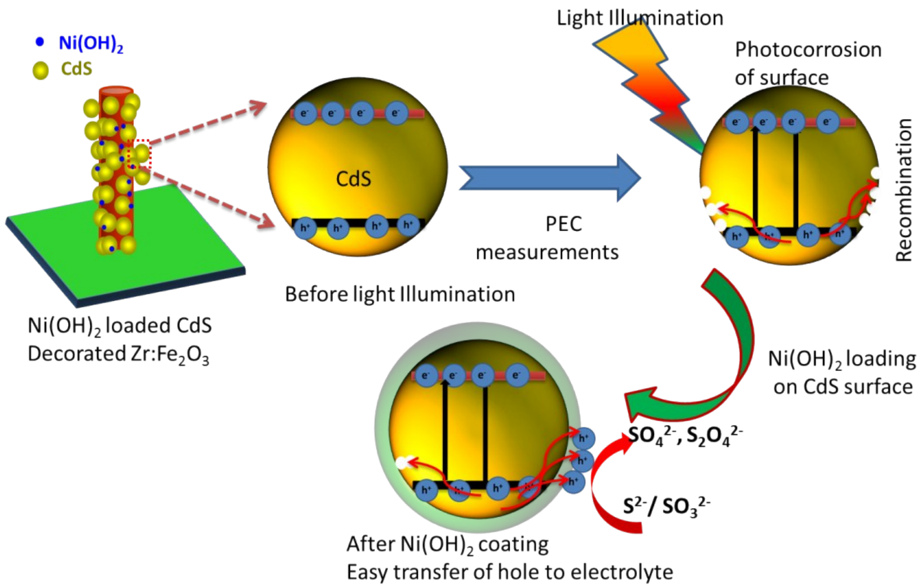

Fig. S12. Schematic presentation of prevention of CdS photo-corrosion by $Ni(OH)_2$ protecting layer.

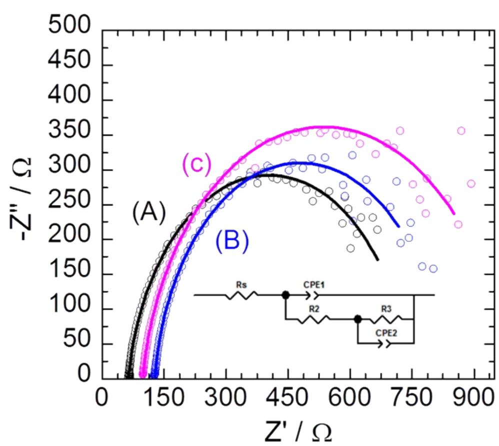

Fig. S13 . EIS Nyquist plots of (A) CdS nanograin-sensitized 1D Zr:α-Fe_2O_3, (B) 5 mM and (C) 10 mM $Ni(OH)_2$ loaded CdS nanograin-sensitized 1D Zr:α-Fe_2O_3 films at -0.3 V vs Ag/AgCl.

References

[1] X. Xie, K. Li, W. D. Zhang, RSC Adv., 2016, **6**, 74234 – 74240.

[2] C. H. Chan, P. Samikkannu and H. W. Wang, Int. J. Hydrogen Energy, 2016, **41**, 17818 – 17825.

[3] J. Tang, J. Li, Y. Zhang, B. Kong, Yiliguma, Y. Wang, Y. Quan, H. Cheng, A.M. Al-Enizi, X. Gong, G. Zheng, Anal. Chem., 2015, **87**, 6703 – 6708.

[4] G. Yang, B. Yang, T. Xiao, Z. Yan, Appl. Surf. Sci., 2013, **283**, 402– 410.

[5] J. H. Bang, P. V. Kamat, Quantum Dot Sensitized Solar Cells. ACS Nano, 2009, **3**, 1467–1476.

[6] P. Sheng, W Li, J. Cai, X. Wang, X. Tong, Q. Cai, C. A. Grimes, J. Mater. Chem. A, 2013, **1**, 7806 – 7815.